Structural Order and Thermal Behavior of Ph-BTBT-10 Monolayer Phases

Structural order and thermal behavior of Ph-BTBT-10 monolayer phases

Elena Ferrari,[*,†,‡] Lorenzo Pandolfi,[¶] Guillaume Schweicher,[§] Yves Geerts,[§,‖] Tommaso Salzillo,[¶] Matteo Masino,[*,†] and Elisabetta Venuti[¶]

†*Dipartimento di Scienze Chimiche, della Vita e della Sostenibilità Ambientale & INSTM-UdR Parma, Parco Area delle Scienze, 17/A, 43124, Parma, Italy*

‡*IMEM-CNR, Parco Area delle Scienze, 37/A 43124 Parma, Italy*

¶*Dipartimento di Chimica Industriale "Toso Montanari" & INSTM-UdR Bologna, Viale del Risorgimento 4 - 40136, Bologna, Italy*

§*Laboratoire de Chimie des Polymères Faculté des Sciences Université Libre de Bruxelles (ULB), Boulevard du Triomphe, CP 206/01, Brussels 1050, Belgium*

‖*International Solvay Institutes of Physics and Chemistry Université Libre de Bruxelles (ULB), Boulevard du Triomphe, CP 206/01, Brussels 1050, Belgium*

E-mail: elena.ferrari@imem.cnr.it; matteo.masino@unipr.it

Abstract

An IR and Raman spectroscopy investigation is carried out on single crystals of the organic semiconductor Ph-BTBT-10 subjected to thermal cycling through the boundaries of its SmE and SmA liquid crystal phases, gaining insight on their structural order. IR measurements in polarized light provide a precise description of both the orientational order of the molecule BTBT rigid cores and the conformational status of its substituents in the mesophases, and shed light on the processes occurring at the phase transitions. The Raman mapping of the crystals obtained in the reverse SmE to

crystal transition reveals the presence of a distinctive polycrystallinity pattern in the recovered samples, an effect which may contribute to the understanding of the variation of the charge carrier mobility of devices experiencing thermal annealing processes

Introduction

Compounds for organic electronics comprise an interesting class of semiconductor materials whose properties derive from the π conjugation induced by their rigid planar molecular structures. Flexible substituents can be introduced by molecular design to enhance their solubility, while crystal engineering modulates packing patterns to optimize the intermolecular interactions that regulate their charge transport characteristics. Due to the large variety of possible assembly patterns in their condensed phases, the formation of different crystalline polymorphs and liquid crystal mesophases is often observed, so that the understanding of the structural and transformation properties of the various phases is a critical step in the quest for the optimal electric performance conditions of these systems.

The molecule 7-decyl-2-phenyl[1]benzothieno[3,2-b][1]benzothiophene (Ph-BTBT-10) has recently gained prominence in the area of organic electronics because of its excellent charge carrier mobility in the crystal state, combined with high chemical stability.[1,2] Its structure, which consists of a stiff Ph-BTBT core connected to a flexible decyl chain (Figure 1a), results in good solubility in organic solvents as well as organized liquid crystal mesophases.[3] In particular, a monoclinic crystal phase is stable up to 150 °C, where it transforms into the Smectic E (SmE), which then transforms into the Smectic A (SmA) at 215 °C; finally, melting occurs at 225 °C.[3] The SmE phases is also known as Crystal E because of its 3D order.

Crystal and liquid crystal phases have distinctive molecular arrangements. The crystal has a bilayer structure, with molecules belonging to adjacent layers stacked head-to-head.;[4] the SmE phase is instead organized in monolayers, with molecules arranged in a head-to-tail fashion.[5,6]

Previous works[7,8] suggested that the crystal to SmE transition takes place through the interpenetration of neighboring layers by collective interlayer molecular translations. In a recent micro-Raman investigation, we gave clear evidence for such a mechanism, demonstrating that the transition occurs by the intervention of a preparatory stage during which the layer interpenetration is driven by an effective lattice phonon, which softens on approaching the phase boundary.[9] Such a stage is followed by the abrupt in plane re-arrangement of the BTBT cores in the herringbone packing of the mesophase. In this work we contribute to the understanding of the structural order of the Ph-BTBT-10 mesophases, and their relationship with the crystal phase, by investigating the vibrational dynamics of Ph-BTBT-10 bulk samples in all its phases.

Polarized mid-IR spectroscopy has been widely used to probe both the molecular orientation and conformation in crystals and thin films[10–12] and is applied here to separately study the temperature evolution of the in-plane orientation order of the Ph-BTBT cores and the conformational order of the decyl chains. Raman mapping in polarized light can provide information on crystal order and domain arrangement of a sample. Applied to the Ph-BTBT-10 crystals recovered by fast and slow cooling of the SmE phase has allowed for the investigation of the features of the re-crystallization process, clarifying the effects of the thermal treatments. Because the array of processes involved in the transformations between the different phases guides the manufacturing of the Ph-BTBT-10 polycrystalline films for organic electronic applications,[1,2,13,14] such a knowledge is in fact crucial.

Results and discussion

The crystal phase

The analysis of the Ph-BTBT-10 mesophases must necessarily start from the understanding of the vibrational properties of the crystal. The typical morphology of the single crystal is platelet-like, with strongly preferred orientation on the ab plane of its $P2_1/a$ monoclinic

structure.[4] The *ab* plane is parallel to the molecular layers and nearly perpendicular to the long Ph-BTBT-10 molecular axis (Figure S2), and the *a* and *b* crystal axes coincide with the two in-plane extinction directions in cross-polarization, as shown in Figure S3. This morphology is therefore suitable for in-plane polarized IR measurements in the transmission mode.

The rigid core and alkyl chain that comprise the Ph-BTBT-10 molecule exhibit different degrees of flexibility, conformational freedom, and intermolecular interaction patterns, resulting in distinct dynamics and thermal behavior. The in-plane orientational order of the cores and the conformational order of the chains can be probed independently by detecting the intramolecular vibrations of the former in the 700-1500 cm^{-1} range and the aliphatic C-H stretching modes of the latter in the 2800-3000 cm^{-1} range. A more detailed assignment of the main bands has been made by comparison of the calculated IR spectrum of an isolated Ph-BTBT-10 molecule with the experiments carried out on the crystalline powder, as shown in Figure 1c where the correlation between isolated molecule and crystal modes is drawn. The match between the two spectra is satisfying, allowing for the identification of the strongest bands, whose corresponding eigenvectors are reported in Figure S1. Note that in the crystal the *a* and *b* polarized components occur at slightly different frequencies as they correspond to two different IR active combinations of the same intramolecular vibrations of the Z=4 molecules in the Ph-BTBT-10 $P2_1/a$ unit cell. Their energy differences arise from the weak interactions between the molecules of the cell.

The spectrum of the powder is richer in bands than the crystal *ab* in-plane polarized spectra, displaying, for instance, strong features around 1460 cm^{-1} . The analysis of the eigenvector calculated at 1445 cm^{-1} shows that these vibrations occur mainly along the long molecular axis, explaining their weak in-plane intensity.

The spectra of Figure 1c also reveal that the relative strengths of the Ph-BTBT core vibrations in the crystal *a* and *b* polarized spectra differ. The in-plane ring stretching modes, which fall in the 1200-1500 cm^{-1} range, are stronger in the *a* polarization; on the contrary,

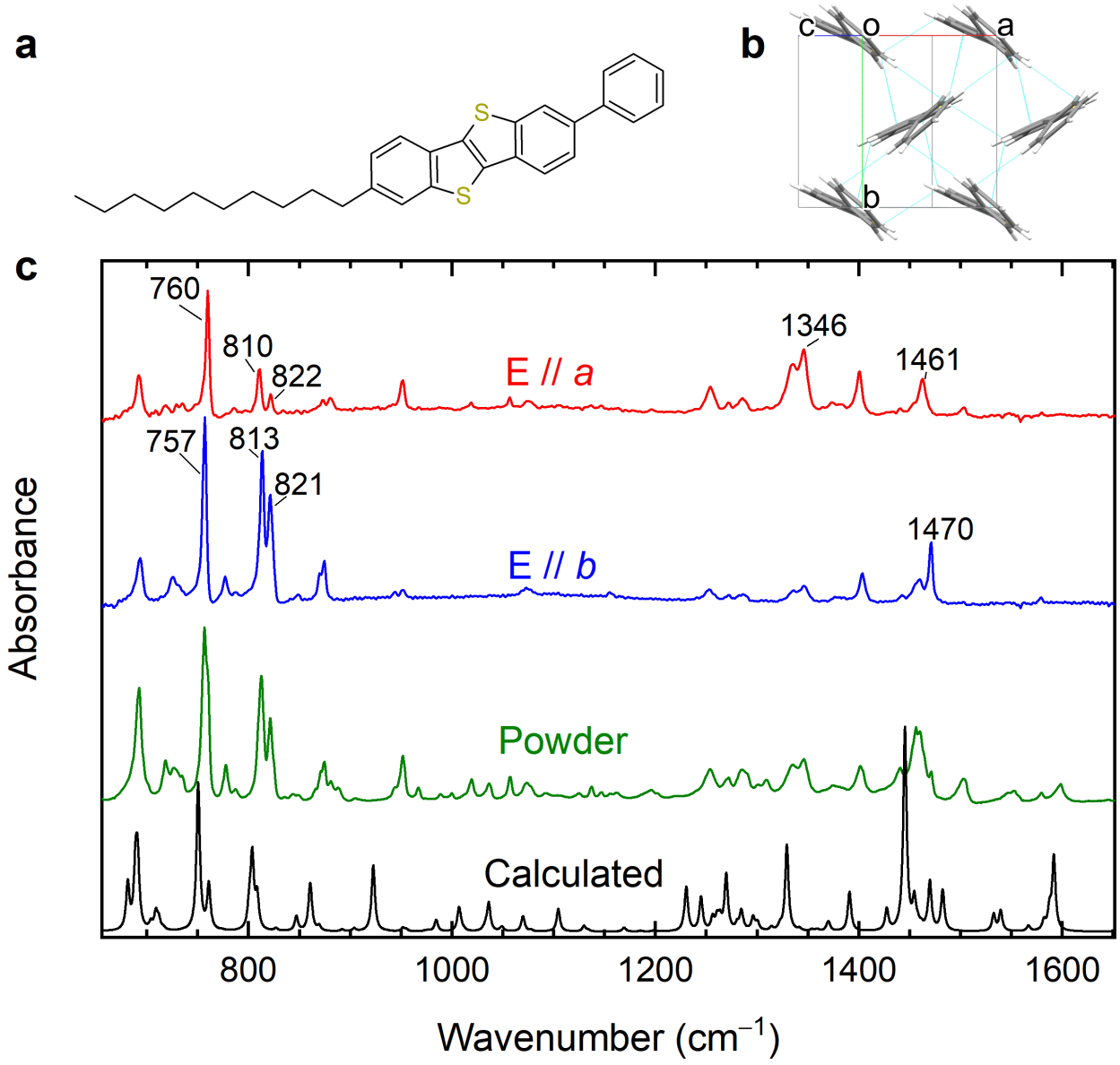

Figure 1: a) Ph-BTBT-10 molecular structure b) Herringbone packing of the Ph-BTBT cores viewed perpendicular to the *ab* plane c) Comparison between the in-plane polarized IR spectra of a Ph-BTBT-10 crystal, the spectrum of the powder and the calculated IR spectrum. The calculated frequencies have been scaled by the factor 0.97.

the out-of-plane C-H bendings of the BTBT group, observed at 812 and 821 cm^{-1} , display higher intensity in the b polarization; finally, the band at 758 cm^{-1} , which is assigned to a phenyl out-of plane C-H bending, has similar intensity in both spectra. These IR intensities are fully consistent with the reported structural determination for the system's aromatic group orientation,[4] with the planes containing the BTBT cores and the phenyl groups inclined by 24° and 44° with respect to the b crystal direction, respectively (Figure 1b).

To complete the assignment of the most relevant peaks, the b polarized narrow band located at 1470 cm^{-1} was ascribed to the chain CH_2 scissoring mode. Noticeably, also the aliphatic C-H stretching modes were found to display higher intensity in the b polarization (Figure 2).

The smectic phases

As shown in Figure 2, the modes assigned to Ph-BTBT-10 cores remain almost unchanged as the temperature increases approaching the SmE phase boundary, whereas the C-H chain vibrations at 1470 cm^{-1} and in the 2800-3000 cm^{-1} range maintain their polarization properties but exhibit pronounced broadening. However, the occurrence of the crystal to SmE transition is marked by their sudden and complete depolarization. This feature reveals that the chains in the SmE phase are highly disordered, and indeed found in the molten state, in agreement with recent spectroscopic results on Ph-BTBT-10 thin films.[15] Noticeably, this is also a general common feature of mesogens formed during crystal to SmE transitions.[16,17] The core vibrations, on the other hand, exhibit in the SmE relative intensities that are similar to those of the original crystal, demonstrating that the cores retain the same reciprocal orientation. Surprisingly, the phenyl out-of plane C-H bending band at 758 cm^{-1} is now b polarized, implying that the phenyl and the BTBT groups must have become nearly coplanar, contrary to what is seen in the crystal; such orientational order must have long range 3D character, as the transmission IR measurements probe the whole sample volume.

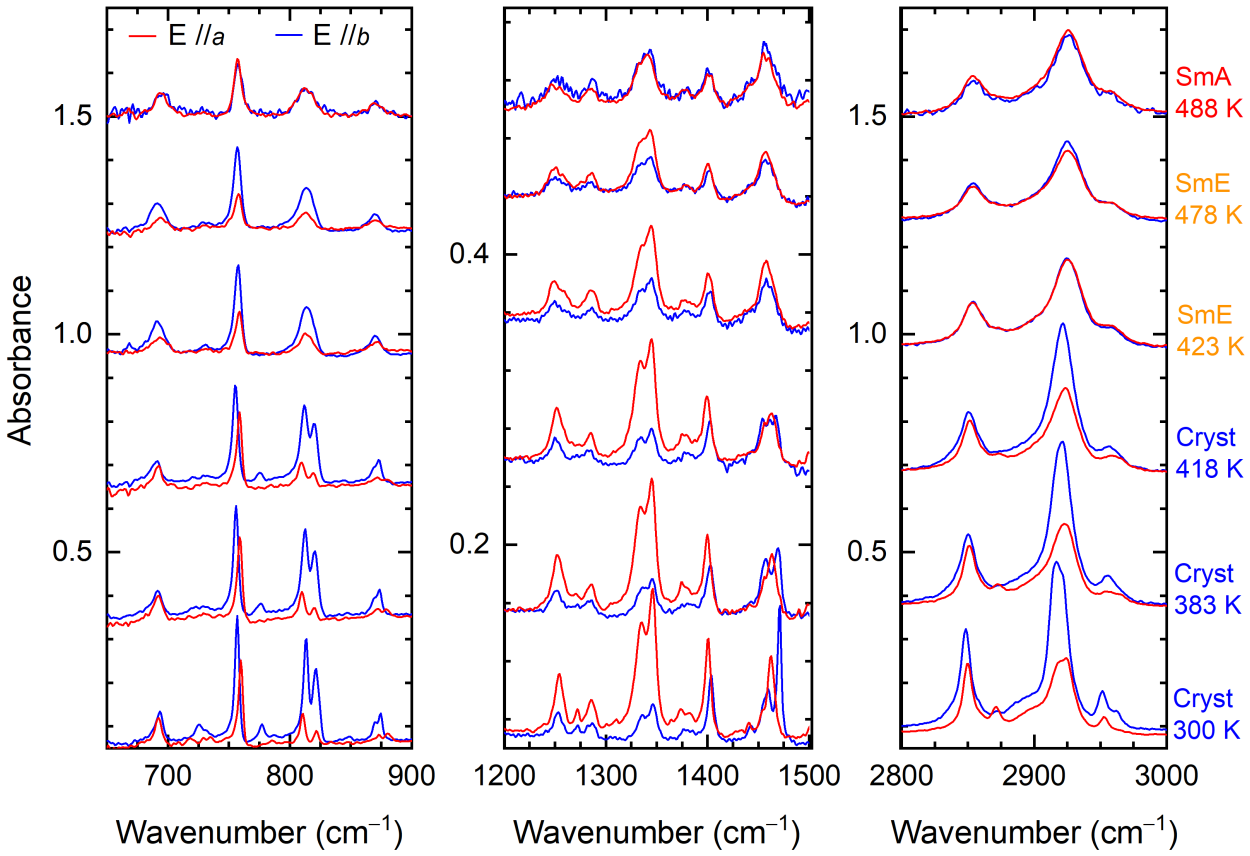

Figure 2: Temperature dependent polarized IR spectra of Ph-BTBT-10, including all its condensed phases (crystal, SmE and SmA). The relevant spectral range has been split into three panels to optimize the choice of the ordinate axis scale. Thus, for the sake of clarity, the spectra are vertically shifted by 0.3 in the left and in the right panel and by 0.1 in the middle panel.

Overall, the spectroscopic features suggest that the SmE phase has a structure which is consistent with the picture of nanosegregation of molten aliphatic chains and in-plane ordered aromatic cores proposed in Refs.,[5,18] contradicting a mixed layer arrangement. In fact, in the SmE the cores assume a herringbone layout as a result of strong π inter-molecular interactions[19] that would be weakened by the presence of intermixed disordered chains. The spectroscopic data also imply that the phenyl and BTBT groups are coplanar, which enhances the π interactions between neighboring units in the antiparallel alignment of the molecules in the mesogen.

On the other hand, based on the characteristics of the SmE phase, head-to-tail disorder must also be present. In the herringbone packing with molecules arranged antiparallel, four distinct orientations are still possible, owing to two molecular long axis alignments and two in-plane core orientations, akin to the crystal phase. The presence of only two molecules in the SmE unit cell[5] indicates a lack of periodicity between adjacent layers and/or within the same layer. It is also worth noting that the correlation in the interlayer direction is likely to be short range, being the layers separated by fluid slabs of disordered chains. A molecular displacement compatible with both the in-plane orientational order and the head-to-tail disorder is the in-plane diffusion described in Ref.[20] Such a picture explains the formation of the monolayer structure without introducing the upside down flipping of the molecules about their short axes. Although described in other SmE mesogens[21] this kind of motion must result hindered in a closely packed phase such as that of Ph-BTBT-10, where a stable in-plane orientational order is maintained.

The IR spectra of the SmE phase in the energy interval of the core vibrations do not undergo depolarization (Figure 2, central panel), either over time or in the entire range of existence of this phase up to 480 K, demonstrating the high stability of its in-plane structural order.

However, the bands of the core vibrations suddenly depolarize at the SmE to SmA transition, which occurs at 488 K. Each doublet merges into one single band whose intensity

corresponds to the average of the polarized spectra of the SmE phase. These observations indicate that whereas the in-plane orientational order is finally lost, the long molecular axes maintain their alignment with respect to the layer normal. Such spectral features are typical of SmA phases, where the molecules can freely rotate about their long axes, are oriented only on average in the same direction and are loosely associated into layers. Diffusion takes freely place between layers and the phase is fluid. Thus, the structural order of the Ph-BTBT-10 crystal is lost step by step through the two smectic phases.

Recrystallization of the SmE phase

As shown in the literature,[22] the observed transitions are reversible, but when the SmE phase is cooled below the crystal transition temperature, the resulting phase and structural order are strongly dependent on the cooling rate. Fast cooling (rate >> 20 K/min) completely suppresses the recrystallization, yielding a glassy solid which is metastable at room temperature.[3] The vitrification of the SmE phase is not clearly detectable under the microscope, as the sample shape is unchanged and no cracks appear on cooling from 423 to 300 K, as shown in the sequence of optical images of Figure S4a. As can be gathered by comparing Figures S3 and S4b (middle panel) the glass is optically uniform as at high temperature, i.e. in the range of SmE thermodynamic stability, and surprisingly it shows over a selected sample area a complete extinction in cross polarization along the same directions of the parent single crystal. Extinction does not occur (Fig S4b, right panel) if the sample is randomly oriented. The IR spectra for the glass at 300 K are given in Figure 3, and they also appear nearly unchanged with respect to those of SmE in its stability range, being characterized by the same polarization properties. Therefore, the glassy solid has the same symmetry and 3D order of the SmE phase; however, most thermal motions present in the SmE phase are expected here to be hindered, so that the dynamic disorder is frozen into a static one.

Thermal annealing of the frozen SmE phase at 393 K results in crystallization, and the parent crystal IR spectral characteristics are entirely restored after 3 hours at this temper-

ature, as illustrated in Figure 3. As reported in the literature,[3,23] slow cooling of the SmE phase also results in the formation of the crystal, which occurs at around 390 K with a cooling rate < 2K/min.[3,23]

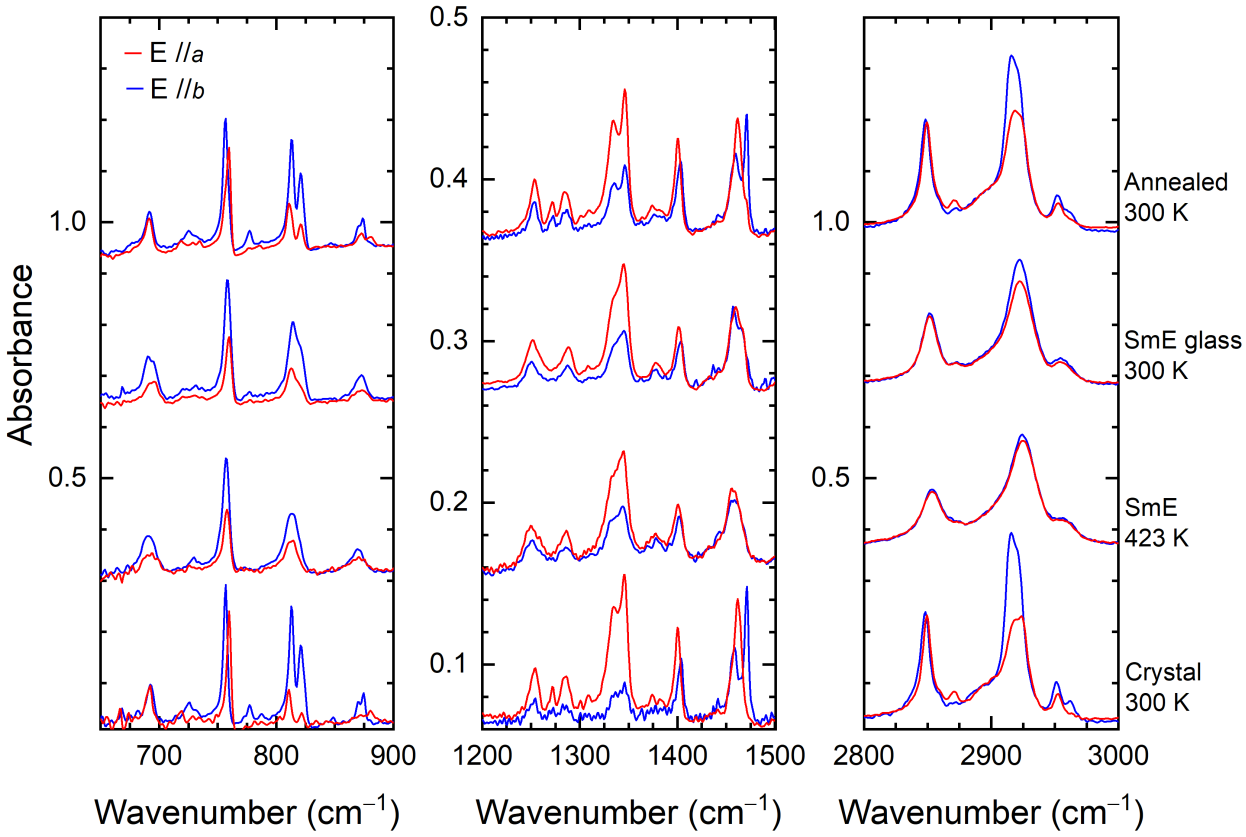

Figure 3: Polarized IR spectra of Ph-BTBT-10. The sample was first heated above the Crystal to SmE transition (SmE), then cooled to 300 K at 90 K/min (SmE glass), then annealed for three hours at 393 K and finally cooled to 300 K (Annealed). In this case annealing yielded a single crystal domain with the same orientation of the pristine crystal, as shown in Figure S6. The spectral range of interest has been split into three panels in order to optimize the choice of the ordinate axis scale. For the sake of clarity, the spectra are upshifted by 0.3 in the left and in the right panel and by 0.1 in the middle panel.

In this case the reverse transition is frequently associated with the sudden formation of surface cracks that extend into the bulk of the sample, in correspondence with the pristine (110) and (1$\bar{1}$0) crystal directions. In fact, the cracks are found to separate crystal domains with different *ab* in-plane orientations. This can be verified by rotating the sample between two crossed polarizers, as extinction occurs at different angles in each domain, unlike what observed when the SmE sample is subjected to fast cooling, as can be clearly seen from

Figures S5 and S7).

As illustrated in Figure 4a, the orientation of the domains was investigated by polarized spectral Raman mapping of a small area containing a few cracks. The collected maps clearly indicate that the in-plane rotation angle is the same in each domain. More detailed Raman measurements with different polarizations detected rotation angles of 0, $\pm 52^{\circ}$ and 90° with respect to the starting crystal reference frame, as can be seen in Figure 4b.

The comparison between the low frequency Raman spectra of a pristine crystal and a recrystallized sample allowed estimating the structural order of the latter, as the lattice phonons detected in this range are expected to be much more sensitive to packing details than the intramolecular vibrations. Indeed, whereas the intramolecular bands fully recover their shape and width regardless of the thermal history, after re-crystallization the lattice phonons are always broader than in the pristine crystal at room temperature. Besides, the faster the recrystallization process, the broader the bands of the retrieved sample (Figure 5). As expected, the extinction in cross-polarization in the recrystallized sample is incomplete at all angles. These spectral feature suggest the presence of a residual structural disorder in the recovered phase, which is consistent with a partial misalignment of the molecules along the c axis.[23] At the same time, the non-random cracking pattern and rotation angles between domains reflect the ordered herringbone arrangement of the starting SmE phase.

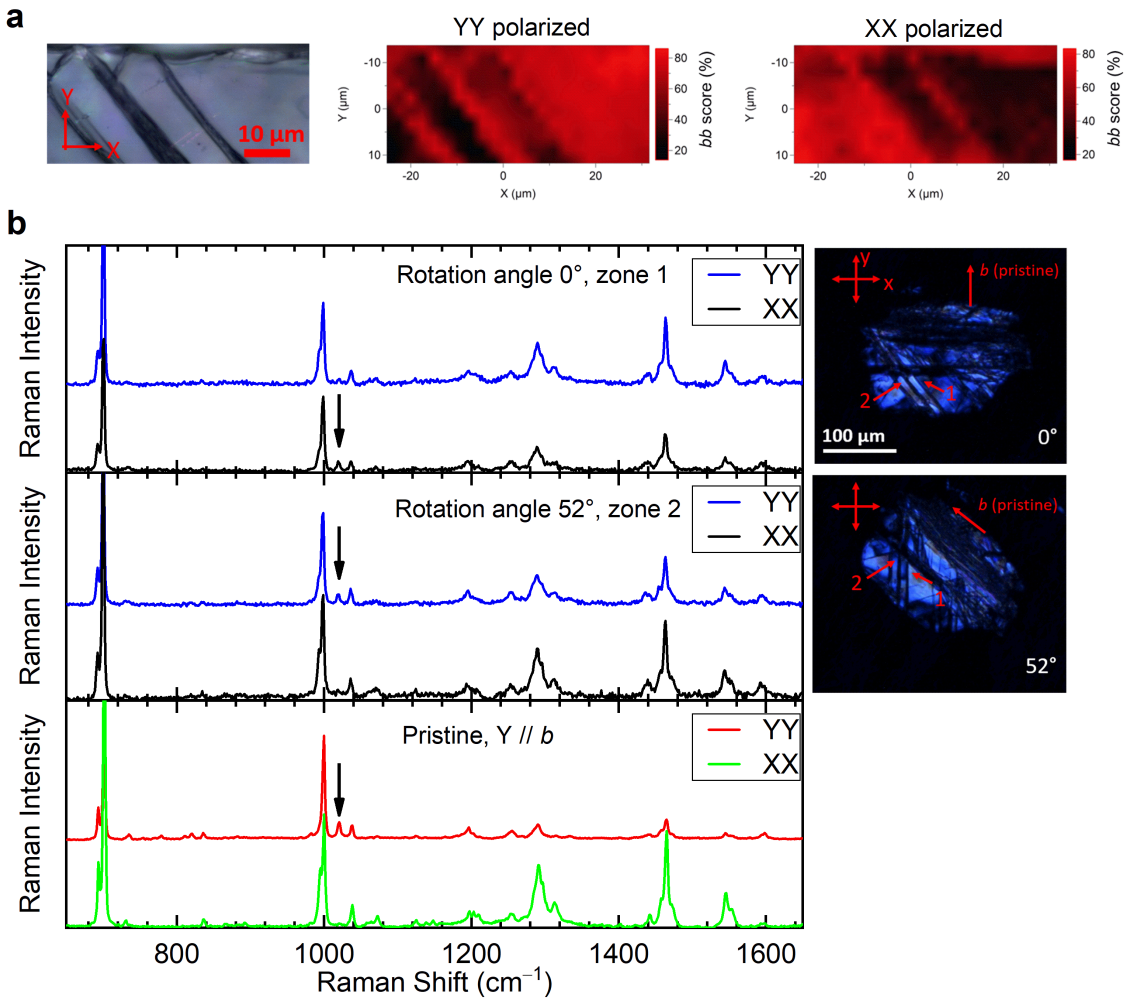

Figure 4: a) Microscopic image of a Ph-BTBT-10 sample obtained by cooling the SmE phase at 1 K/min, with the corresponding YY and XX polarized Raman maps. The spectra measured in each point were fitted with a linear combination of the *aa* and *bb* polarized spectra of an untreated single crystal, shown in b), lower panel. The intensity of the red colour represent the normalized weight assigned to the *bb* polarized spectrum. b) Comparison between the polarized Raman spectra recorded on a pristine crystal (lower panel) and on a recrystallized sample (upper and middle panels), in the two domains indicated in the images on the right. Both the exciting and scattered light are polarized along X or Y. The in-plane orientation of the domains is recognized comparing the observed spectra with the reference polarized spectra shown in the lower panel. The sample was rotated to maximize the difference between the XX and YY polarized spectra in the two domains, to find their orientation. The a and b axes are rotated by 90° in domain 1 and 52° in domain 2 respect to the pristine crystal. The black arrow indicates a band visible only with *bb* polarization

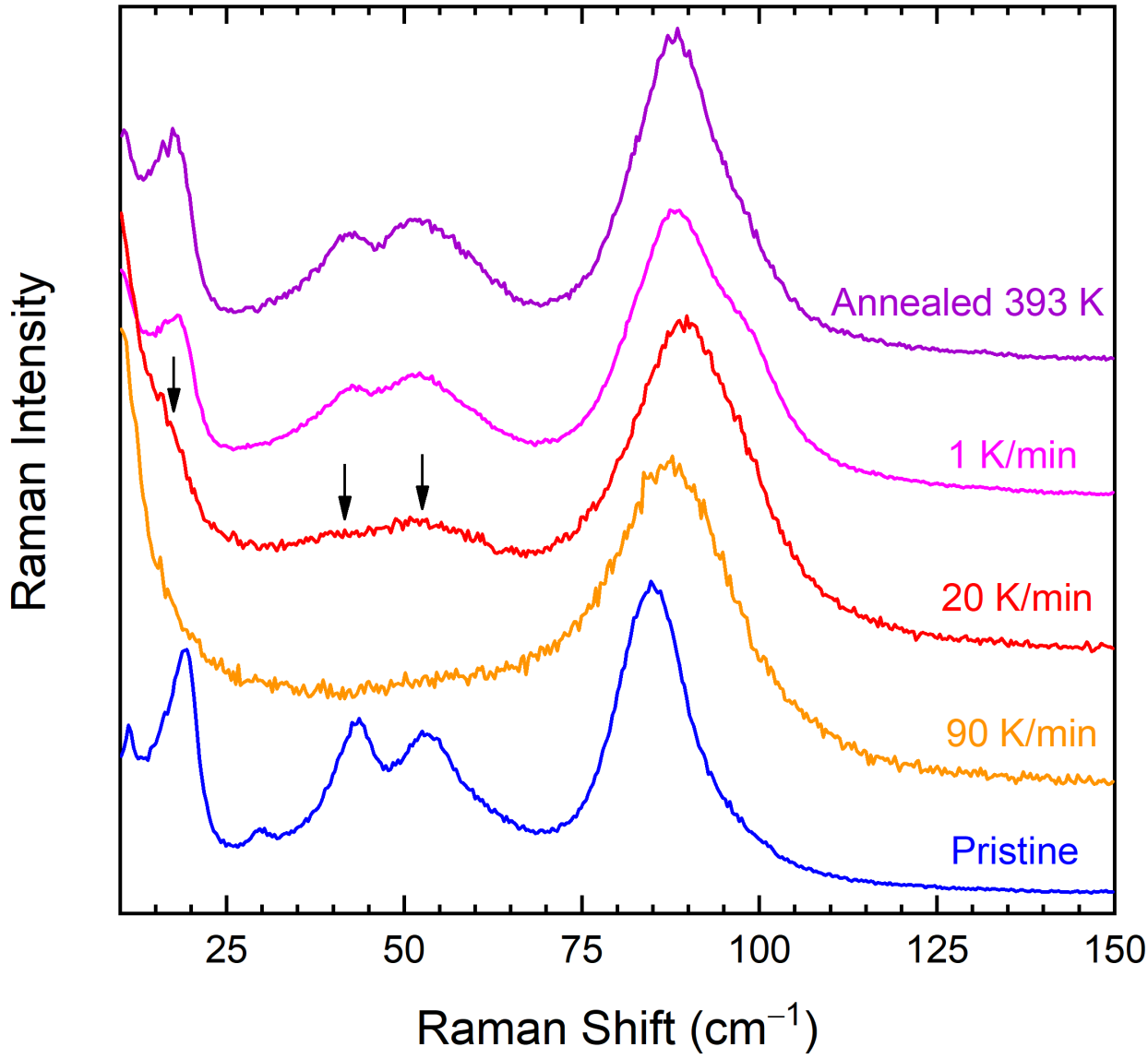

Figure 5: Comparison between the low frequency Raman spectra of Ph-BTBT-10 after different thermal treatments. The sample cooled at 90 K/min belongs to the frozen SmE phase. The black arrows mark three phonon bands indicating the recrystallization. All the spectra are *bb* polarized: when necessary the samples were rotated to achieve the required orientation.

Conclusions

In summary, in this work the spectroscopic study of the temperature transitions undergone by Ph-BTBT-10 crystals allowed to identify the temperature induced changes in molecular orientation and packing which characterise the compound liquid crystal phases.

The employment of bulk specimens allowed the investigation of the properties of the material without the influence of the interaction with a substrate, and we believe that the obtained results are fully transferable to Ph-BTBT-10 thin films, in which the same phases appear and are stable over the same temperature intervals. The long range orientational order of the SmE phase, which shares the same in-plane symmetry axes as the parent crystal phase, was first confirmed, proving that the vertical alignment of the molecules and the layer orientation are also conserved. These data support the suggested mechanism for the crystal to SmE, which involves collective interlayer molecular translations. The in-plane rearrangement of the cores which follows leads the anti-parallel aligned molecules to a new herringbone order. Most importantly, the changes in the polarization properties of the system reveals that the transition is associated with the melting of the decyl chains and the co-planarization of the phenyl and BTBT units, a rearrangement that take places owing to the segregation of cores and chains in the SmE phase. The evolution of the IR polarized spectra in temperature also identifies the structural changes that accompany the transition from SmE to SmA liquid crystal phases.

All Ph-BTBT-10 temperature transitions are reversible. However, the crystallinity of the material resulting from the SmE to crystal transformation is strongly dependent on its thermal treatment. The normal to the molecular layers remains unchanged from one phase to the other, but in the backward transition the two a an b in-plane axes may get rotated with respect to the starting ones, giving evidence of the occurrence of molecular rotations about the long axis. This results in the formation of many different crystal domains with a ab mosaicity in the recovered sample, which is clearly highlighted by the Raman maps. The molecular rearrangements that restore the crystal interaction patterns must follow the layer

interpenetration, as in the case of the Crystal to SmE process. The transition mechanism is therefore similar in both directions, but the partial disorder in the SmE phase results in a polycrystalline recrystallized sample. Thermal cycling through the phase boundary is expected to enhance the polycrystallinity, and the safest way to recover the characteristics of the pristine crystal state appear, healing the disorder induced by the formation of the mesophase, appear to be a long annealing process of the frozen SmE.

Experimental

Ph-BTBT-10 synthesis and crystal growth

Ph-BTBT-10 was synthesized following the previously reported procedure.[3] Single crystals were grown by recrystallization of the synthesized powder in 1,2-dichlorobenzene. The crystals are very thin platelets with typical size 100 x 200 x 5 μm^3 (Figure S2). Single crystal domains were selected for the measurements by polarized optical microscopy.

Spectroscopic measurements

The polarized IR spectra were measured in transmission mode on single crystals laying on the *ab* plane placed on a ZnSe slide, using a Bruker IFS-66 FT-IR spectrometer coupled to a Hyperion 1000 IR microscope.

The Raman spectra and spectral maps were acquired with a Horiba Lab RAM HR Evolution Raman microscope, exciting with the 633 nm line. Raman confocal microscopy, differently from IR, allows to probe the different domains selectively due to the increased spatial resolution. Depending on the diffraction limit and the optics of the microscopes, the spot size is around 500 nm in Raman and 50-100 μm in IR.

Raman measurements were performed in backscattering geometry with the exciting and scattered light linearly polarized along either the X (horizontal) or Y (vertical) directions of the laboratory reference system. The crystals were oriented with the *b* axis aligned with the

Y direction. The spectral maps were acquired on the samples recrystallized from a starting SmE phase, to probe the in-plane orientation of the crystal axes with respect to that of the pristine specimen. The lateral step between map grid points was 2 μm. The polarized Raman maps were obtained using the Classical Least Squares algorhytm available in the Horiba LabSpec6 software. The spectra measured on each point were fitted with a linear combination of the pristine *aa* and *bb* polarized spectra, where the two letters indicate the polarization direction of the exciting and scattered light with respect to the crystal axes. The resulting weights were normalized to 100.

The temperature was controlled in the range 300-488 K using a Linkam HFS 91 stage, fitted under the microscopes. SmE phase samples obtained from single crystals were cooled down from 430 K to room temperature at different cooling rates, from 0.5 to 90 K/min. The rapidly cooled samples were then annealed 3h at 393 K, to follow the cold crystallization of the glassy SmE phase.

Calculations

Standard DFT computational methods (B3LYP, 6-311++G**) were employed for the calculation of the equilibrium geometry and vibrational frequencies of the isolated Ph-BTBT-10 molecule, using the Gaussian 16 software.[24] The calculated frequencies were scaled by 0.97 for the comparison with the experimental values.[25]

Acknowledgement

This work has been supported by the project "POLYPHON - Polymorph screening to enable electron-phonon coupling engineering in organic semiconductors" funded by the MUR Progetti di Ricerca di Rilevante Interesse Nazionale (PRIN) Bando 2022 - grant 2022XZ2ZM8. The work has benefited from the equipment and framework of the COMP-HUB Initiative, funded by the 'Departments of Excellence' program of the Italian Ministry for Education,

University and Research (MIUR, 2018-2022). T.S. thanks the Programma per Giovani Ricercatori "Rita Levi Montalcini" year 2020 (grant PGR20QN52R) of the Italian Ministry of University and Research (MUR) for the financial support. Project funded under the National Recovery and Resilience Plan (NRRP), Mission 04 Component 2 Investment 1.5 - NextGenerationEU, call for tender n. 3277 dated 30/12/2021 (award number: 0001052 dated 23/06/2022). Y. G. is thankful to the Belgian National Fund for Scientific Research (FNRS) for financial support through research projects Pi-Chir (No T.0094.22) and CHISUB (No 40007495). G. S. is a FNRS Research Associate. G.S. acknowledges financial support from the Francqui Foundation (Francqui Start-Up Grant). G.S. thanks the FNRS for financial support through research project COHERENCE2 (N° F.4536.23).

Supporting Information Available

DFT calculated eigenvectors of selected vibrational modes of the Ph-BTBT-10 isolated molecule, Ph-BTBT-10 unit cell representation, microscopic images of the crystal morphology in bright field and in crossed polarizers configuration taken after the different thermal processes.

References

(1) Iino, H.; Hanna, J.-i. Liquid crystalline thin films as a precursor for polycrystalline thin films aimed at field effect transistors. *Journal of Applied Physics* **2011**, *109*, 074505.

(2) Iino, H.; Kobori, T.; Hanna, J.-i. Improved thermal stability in organic FET fabricated with a soluble BTBT derivative. *Journal of non-crystalline solids* **2012**, *358*, 2516–2519.

(3) Iino, H.; Usui, T.; Hanna, J.-i. Liquid crystals for organic thin-film transistors. *Nature Communications* **2015**, *6*, 6828.

(4) Minemawari, H.; Tsutsumi, J.; Inoue, S.; Yamada, T.; Kumai, R.; Hasegawa, T. Crystal structure of asymmetric organic semiconductor 7-Decyl-2-phenyl[1]benzothieno[3, 2 − *b*][1]benzothiophene. *Applied Physics Express* **2014**, *7*, 091601.

(5) Hofer, S.; Bodlos, W.; Novák, J.; Sanzone, A.; Beverina, L.; Resel, R. Molecular packing analysis of the crystal smectic E phase of a benzothieno-benzothiophene derivative by a combined experimental / computational approach. *Liquid Crystals* **2021**, *48*, 1888–1896.

(6) Iino, H.; Hanna, J.-I. Liquid crystal and crystal structures of a phenyl-benzothienobenzothiophene derivative. *Molecular Crystals and Liquid Crystals* **2017**, *647*, 37–43.

(7) Yoneya, M. Monolayer Crystal Structure of the Organic Semiconductor 7-Decyl-2-phenyl[1]benzothieno[3, 2 − *b*][1]benzothiophene. *The Journal of Physical Chemistry C* **2018**, *122*, 22225–22231.

(8) Yoneya, M. Monolayer crystal structure of the organic semiconductor 7-Decyl-2-phenyl[1]benzothieno[3, 2 − *b*][1]benzothiophene, revisited. *Japanese Journal of Applied Physics* **2020**, *59*, 090909.

(9) Ferrari, E.; Pandolfi, L.; Schweicher, G.; Geerts, Y.; Salzillo, T.; Masino, M.; Venuti, E. Interlayer Sliding Phonon Drives Phase Transition in the Ph-BTBT-10 Organic Semiconductor. *Chemistry of Materials* **2023**, *35*, 5777–5783.

(10) Majewska, P.; Rospenk, M.; Czarnik-Matusewicz, B.; Kochel, A.; Sobczyk, L.; Dabrowski, R. X-ray diffraction, DFT theoretical, and IR polarized spectroscopic studies of the crystal-like E-mesophase of 4'-hexyloxy-isothiocyanatotolane (6OTOLT). *Chemical Physics* **2007**, *340*, 227–236.

(11) Jasiurkowska, M.; Ściesiński, J.; Czub, J.; Massalska-Arodź, M.; Pełka, R.; Juszyńska, E.; Yamamura, Y.; Saito, K. Infrared Spectroscopic and X-ray Studies of

the 4-Propyl-4'-isothiocyanatobiphenyl (3TCB). *The Journal of Physical Chemistry B* **2009**, *113*, 7435–7442.

(12) Jasiurkowska, M.; Zielinski, P. M.; Massalska-Arodź, M.; Yamamura, Y.; Saito, K. Study of polymorphism of 4-hexyl-4'-isothiocyanatobiphenyl by complementary methods. *The Journal of Physical Chemistry B* **2011**, *115*, 12327–12335.

(13) Wan, J.; Li, Y.; Benson, J.; Miller, R.; Zhernenkov, M.; Freychet, G.; Headrick, R. L. Dynamic processes in transient phases during self-assembly of organic semiconductor thin films. *Mol. Syst. Des. Eng.* **2022**, *7*, 34–43.

(14) Tamayo, A.; Hofer, S.; Salzillo, T.; Ruzié, C.; Schweicher, G.; Resel, R.; Mas-Torrent, M. Mobility anisotropy in the herringbone structure of asymmetric Ph-BTBT-10 in solution sheared thin film transistors. *Journal of Materials Chemistry C* **2021**, *9*, 7186–7193.

(15) Shioya, N.; Yoshida, M.; Fujii, M.; Shimoaka, T.; Miura, R.; Maruyama, S.; Hasegawa, T. Conformational Change of Alkyl Chains at Phase Transitions in Thin Films of an Asymmetric Benzothienothiophene Derivative. *The Journal of Physical Chemistry Letters* **0**, *0*, 11918–11924, PMID: 36525547.

(16) Inoue, S.; Minemawari, H.; Tsutsumi, J.; Chikamatsu, M.; Yamada, T.; Horiuchi, S.; Tanaka, M.; Kumai, R.; Yoneya, M.; Hasegawa, T. Effects of Substituted Alkyl Chain Length on Solution-Processable Layered Organic Semiconductor Crystals. *Chemistry of Materials* **2015**, *27*, 3809–3812.

(17) Yamamura, Y.; Adachi, T.; Miyazawa, T.; Horiuchi, K.; Sumita, M.; Massalska-Arodź, M.; Urban, S.; Saito, K. Calorimetric and Spectroscopic Evidence of Chain-Melting in Smectic E and Smectic A Phases of 4-Alkyl-4'-isothiocyanatobiphenyl (nTCB). *The Journal of Physical Chemistry B* **2012**, *116*, 9255–9260, PMID: 22765025.

(18) Yamamura, Y.; Murakoshi, T.; Hishida, M.; Saito, K. Examination of molecular packing in orthogonal smectic liquid crystal phases: a guide for molecular design of functional smectic phases. *Physical Chemistry Chemical Physics* **2017**, *19*, 25518–25526.

(19) Saito, K.; Miyazawa, T.; Fujiwara, A.; Hishida, M.; Saitoh, H.; Massalska-Arodź, M.; Yamamura, Y. Reassessment of structure of smectic phases: Nano-segregation in smectic E phase in 4-n-alkyl-4'-isothiocyanato-1, 1'-biphenyls. *The journal of chemical physics* **2013**, *139*, 114902.

(20) Vaz, N. A.; Vaz, M. J.; Doane, J. W. Molecular ordering and motion within the smectic-E phase: H 2 NMR study. *Physical Review A* **1984**, *30*, 1008.

(21) Jasiurkowska, M.; Budziak, A.; Czub, J.; Massalska-Arodź, M.; Urban, S. X-ray studies on the crystalline E phase of the 4-n-alkyl-4'-isothiocyanatobiphenyl homologous series (nBT, n = 2–10). *Liquid Crystals* **2008**, *35*, 513–518.

(22) Baggioli, A.; Casalegno, M.; Raos, G.; Muccioli, L.; Orlandi, S.; Zannoni, C. Atomistic Simulation of Phase Transitions and Charge Mobility for the Organic Semiconductor Ph-BTBT-C10. *Chemistry of Materials* **2019**, *31*, 7092–7103.

(23) Hofer, S.; Unterkofler, J.; Kaltenegger, M.; Schweicher, G.; Ruzié, C.; Tamayo, A.; Salzillo, T.; Mas-Torrent, M.; Sanzone, A.; Beverina, L.; Geerts, Y. H.; Resel, R. Molecular Disorder in Crystalline Thin Films of an Asymmetric BTBT Derivative. *Chemistry of Materials* **2021**, *33*, 1455–1461, PMID: 33642680.

(24) Frisch, M. J. et al. Gaussian˜16 Revision C.01. 2016; Gaussian Inc. Wallingford CT.

(25) Merrick, J. P.; Moran, D.; Radom, L. An Evaluation of Harmonic Vibrational Frequency Scale Factors. *The Journal of Physical Chemistry A* **2007**, *111*, 11683–11700.

TOC Graphic

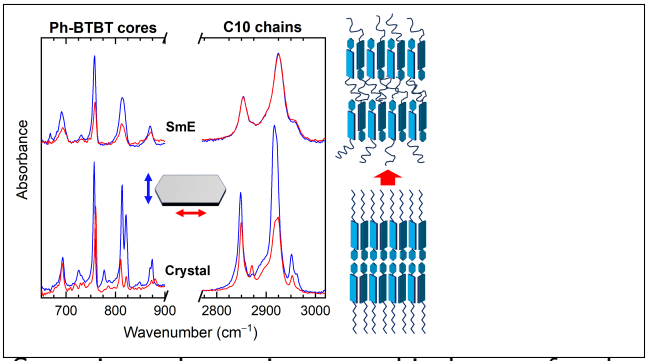

Some journals require a graphical entry for the Table of Contents. This should be laid out "print ready" so that the sizing of the text is correct.

Inside the `tocentry` environment, the font used is Helvetica 8 pt, as required by *Journal of the American Chemical Society*.

The surrounding frame is 9 cm by 3.5 cm, which is the maximum permitted for *Journal of the American Chemical Society* graphical table of content entries. The box will not resize if the content is too big: instead it will overflow the edge of the box.

This box and the associated title will always be printed on a separate page at the end of the document.